

## Thermal equation of state of $\text{CaSiO}_3$ perovskite

Yanbin Wang, Donald J. Weidner, and François Guyot<sup>1</sup>

Center for High-Pressure Research and Department of Earth and Space Sciences, State University of New York at Stony Brook

**Abstract.** A comprehensive pressure-volume-temperature data set has been obtained for  $\text{CaSiO}_3$  perovskite up to 13 GPa and 1600 K, using synchrotron X ray diffraction with a cubic-anvil, DIA-6 type apparatus (SAM-85). For each volume measurement, nonhydrostatic stress is determined from the relative shift in the diffraction lines of NaCl, within which the sample was embedded. Heating to above 973 K greatly reduced the strength of NaCl (to below 0.05 GPa), making the measurements hydrostatic. At room temperature the cubic perovskite structure remains metastable at pressures as low as 1 GPa, below which the sample transforms into an amorphous phase as indicated by a large background, a marked decrease in diffraction signals, and an anomalous volume decrease of the remaining crystalline phase. Because our experimental uncertainties are significantly smaller than those in previous measurements, the new data provide a tighter constraint on the zero pressure bulk modulus for  $\text{CaSiO}_3$  perovskite. A new set of room temperature equation of state parameters are identified so that both our data and the diamond cell data of *Mao et al.* [1989] are compatible [ $K_{T0} = 232(8)$  GPa,  $K'_{T0} = 4.8(3)$ , and  $V_0 = 45.58(4)$  Å<sup>3</sup>]. Volume measurements along several isotherms under both stable and metastable pressure conditions allow isochoric and isobaric interpolations within the range of experimental pressure and temperature conditions. Analyses using various approaches yielded consistent results for  $(\partial K_T/\partial T)_P$  of  $-0.033(8)$  GPa K<sup>-1</sup>, and  $(\partial\alpha/\partial P)_T$  of  $-6.3 \times 10^{-7}$  GPa<sup>-1</sup> K<sup>-1</sup>, with a zero-pressure thermal expansion  $\alpha_0$  of  $3.0 \times 10^{-5}$  K<sup>-1</sup>. The thermal pressure is found to be virtually independent of volume, and thus the Anderson-Grüneisen parameter  $\delta_T = K'_{T0} = 4.8$ . These results are used to predict the bulk modulus and density of  $\text{CaSiO}_3$  perovskite under lower mantle conditions. Along an adiabat with the foot temperature of 2000 K, the density of the perovskite agrees with that of the preliminary reference Earth model (PREM) within 1% throughout the lower mantle. The bulk modulus shows a smaller pressure dependence along the adiabat; it matches that of PREM at the top of the lower mantle but is about 10% too low near the core-mantle boundary.

### Introduction

Mineral physics constraints on the composition of the Earth's lower mantle rely on knowledge of thermal equations of state of candidate minerals. Until recently, pressure-volume-temperature ( $P$ - $V$ - $T$ ) data have been obtained only for  $(\text{Mg,Fe})\text{SiO}_3$  perovskite [*Mao et al.*, 1991; *Wang et al.*, 1994; *Utsumi et al.*, 1995; *Funamori et al.*, 1995] and magnesiowustite [*Fei et al.*, 1992]. Phases containing other major elements such as Ca and Al have not yet been well studied. According to current estimates of the composition of the Earth, an MgO-FeO-SiO<sub>2</sub> system would account for about 90% of the mantle volume, whereas including CaO and Al<sub>2</sub>O<sub>3</sub> components may improve the coverage to 99% [e.g., *Anderson*, 1989].

Several phases have been proposed to be the possible hosts of aluminum in the lower mantle, including NaAlSiO<sub>4</sub> [*Liu*, 1978], MgAl<sub>2</sub>O<sub>4</sub> [*Trifune et al.*, 1991], and Al<sub>2</sub>SiO<sub>5</sub> [*Ahmed-*

*Zaid and Madon*, 1991]. However, these phases were synthesized without the presence of the major lower mantle phases ((Mg,Fe)SiO<sub>3</sub> perovskite and magnesiowustite) and therefore their existence in the lower mantle is questionable on petrological grounds. A recent phase equilibrium study using a more representative composition of the mantle (pyrolite) shows that Al is mostly accommodated in (Mg,Fe)SiO<sub>3</sub> perovskite with no separate aluminous phase observed [*Trifune*, 1994].

On the other hand, a number of other experimental studies indicate that the most likely calcium-bearing phase is CaSiO<sub>3</sub> perovskite [*Ringwood and Major*, 1971; *Liu and Ringwood*, 1975, *Gasparik*, 1989, 1971]. Thus the lower mantle may be composed mainly of aluminous (Mg,Fe)SiO<sub>3</sub> perovskite, CaSiO<sub>3</sub> perovskite, and magnesiowustite, as well as 1 or 2% of other phases.

Equation of state measurements of CaSiO<sub>3</sub> perovskite are complicated by the instability of this material. Thus it is not possible to synthesize the sample in one experiment and conduct high-pressure, high-temperature measurements in another. Rather, the synthesis experiment must be capable of giving equation of state information. Equation of state of CaSiO<sub>3</sub> perovskite has been measured at ambient temperature by several groups in a diamond anvil cell [e.g., *Mao et al.*, 1989; *Tarida and Richet*, 1989; *Tamai and Yagi*, 1989]. *Wang and Weidner* [1994] reported the first in situ determination of the

<sup>1</sup>Also at Institut de Physique du Globe de Paris and Laboratoire de Mineralogie Cristallographie, Université de Paris 7, Paris

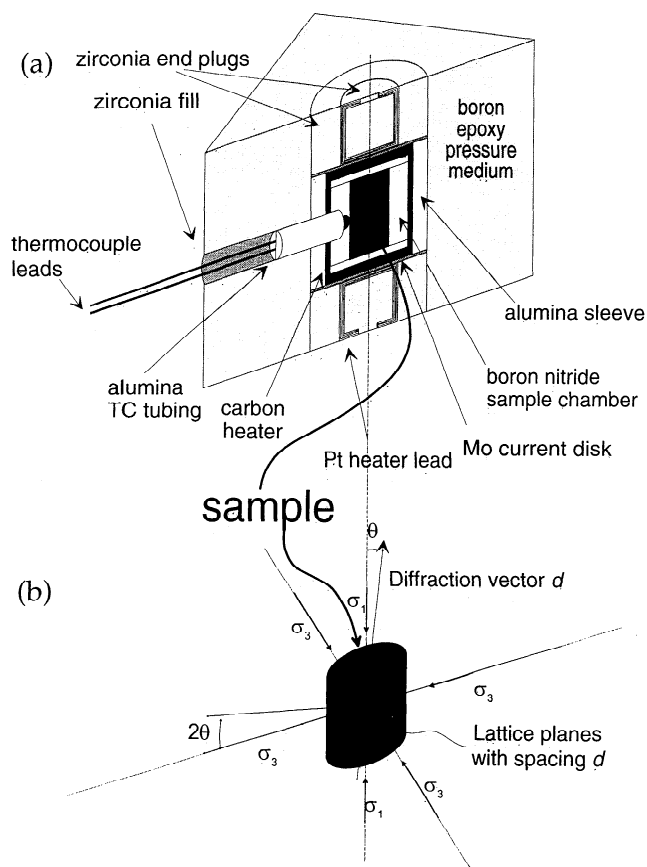


**Figure 1.** Cell assembly used in this study. (a) Cutaway view of the assembly, with sample sandwiched in between two layers of NaCl/BN mixture and thermocouple junction in contact with sample. (b) Approximate stress geometry and relation with diffraction geometry. With a fixed  $2\theta$  of  $7.5^\circ$ , crystal planes that give rise to diffraction signals are approximately parallel to the diffraction vector. Stress geometry is such that the vertical stress component  $\sigma_1$  is different from the horizontal components  $\sigma_2 = \sigma_3$ .

phase boundary between  $\text{CaSiO}_3$  perovskite and the low-pressure phase assemblage  $\text{Ca}_2\text{SiO}_4 + \text{CaSi}_2\text{O}_5$ . They also obtained volume measurements along several nearly isobaric paths up to 1600 K, within the stability field. However, the limited pressure range did not allow a complete determination of the thermal equation of state.

In this paper we extend the work by Wang and Weidner [1994] to examine a more complete thermal equation of state. With better understanding of the nonhydrostatic stress in the system and more precise  $P$ - $V$ - $T$  measurements, we have improved the performance of the cell assembly so that it allows pressure to be varied in a large range, making it possible to measure isothermal compression curves at various temperatures. These data, in combination with those obtained by Wang and Weidner [1994], allow a direct examination of several thermodynamic relations and a determination of the thermal equation of state.

## Experimental Procedure

The high pressure, high temperature experiments were carried out in a DIA-6 type cubic-anvil apparatus (SAM-85) with sintered diamond as anvil material ( $4 \times 4$  mm truncation size).

The apparatus was installed at the superconducting beam line (X17B1) of the National Synchrotron Light Source at Brookhaven National Laboratory, Upton, New York. Details of the apparatus are described by Weidner *et al.* [1992].

Figure 1 shows the sample assembly used in this study. The starting material was synthetic, high-purity wollastonite, the same material used in the study of Wang and Weidner [1994]. A 1.0-mm-diameter, 2.0-mm-long sample chamber was filled with one layer of wollastonite in the middle and two layers of a mixture of NaCl and BN (weight ratio 4:1) on top and bottom of the sample. Both the sample and the NaCl-BN mixture were dried at 570 K for more than 10 h before the experiment. The sample assembly was compressed at room temperature to about 13–14 GPa and heated to above 1400 K in order to synthesize  $\text{CaSiO}_3$  perovskite. Unit cell volume of the perovskite was then measured at various pressure and temperature conditions. Pressure was determined by the thermal equation of state of NaCl [Decker, 1971], and temperature was measured with a W/Re24%-W/Re6% thermocouple. The temperature was generally stable within 1 K up to 900 K and within 5 K to 1600 K. The X ray beam was collimated to  $100 \mu\text{m}$  and  $200 \mu\text{m}$  in the vertical and horizontal dimensions, respectively, and the temperature variation within the diffracting volume is less than 5 K.

The diffraction system was carefully calibrated using the method described by Wang *et al.* [1994]. For  $\text{CaSiO}_3$  perovskite, up to 11 peaks were observed whose  $d$  spacings range from 2.6 to  $0.8 \text{ \AA}$ , making it possible to determine precisely the unit cell parameters. The unit cell volume refinements generally have uncertainties of  $0.02 \text{ \AA}^3$  ( $\sim \pm 0.05\%$ ). An example of the diffraction patterns obtained at high pressure and temperature is shown in Figure 2a.

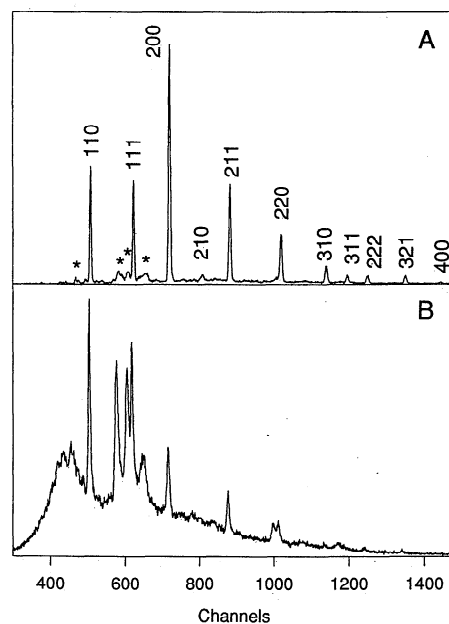


**Figure 2.** Examples of the diffraction spectra of  $\text{CaSiO}_3$  perovskite. (a) Spectrum obtained at 11.7 GPa and 1172 K. A total of 11 diffraction lines are observed. Asterisks indicate diffraction lines from the lower-pressure phase assemblage  $\text{Ca}_2\text{SiO}_4 + \text{CaSi}_2\text{O}_5$ . (b) Pattern collected at 0.59 GPa during decompression at room temperature. Note the drop in peak intensity and the enhanced background due to partial amorphization.

As the specimen is in a solid-medium environment, nonhydrostatic stresses are present, which may significantly affect the volume measurement. *Weidner et al.* [1994] have discussed the characteristics of the stress field in the SAM-85 and the methods to measure the nonhydrostatic stress (also see Figure 1). Briefly, the macroscopic stress field may be approximated as being cylindrical in symmetry, with the vertical stress component ( $\sigma_1$ ) different from the girdle stresses ( $\sigma_2 = \sigma_3$ ). The true pressure is defined as the average of the three principal stress components:  $P = (1/3)(\sigma_1 + 2\sigma_3)$ .

Several related problems arise in determining  $P$ - $V$ - $T$  relations in the presence of nonhydrostatic stresses. (1) The diffraction vector is approximately parallel to  $\sigma_1$ ; only the crystallographic planes that are perpendicular to  $\sigma_1$  will be seen. The true pressure is different from that measured from diffraction of NaCl by approximately  $(K/\mu)\Delta\sigma$ , where  $K$  and  $\mu$  are the bulk and shear moduli of NaCl and  $\Delta\sigma (= \sigma_1 - \sigma_3)$  is the magnitude of the nonhydrostatic stress [*Meng et al.*, 1993]. (2) Similarly, measurements of sample volume are either overestimated or underestimated depending on whether  $\sigma_1$  is smaller or greater than  $\sigma_3$  for a given mean pressure. (3) Under a boundary condition  $\sigma_1 \neq \sigma_3$ , each diffraction line will be shifted relative to the others owing to elastic anisotropy, giving rise to inconsistent cell parameters, resulting in large uncertainties in determination of the cell volume. At this stage, we have not found a satisfactory way to correct the effects of nonhydrostatic stresses in the volume measurement. Thus we choose to discard the data that are contaminated by nonhydrostatic stresses.

We determine the macroscopic nonhydrostatic stresses in NaCl by measuring the relative shift in the diffraction lines of NaCl. The algorithm is outlined by *Weidner et al.* [1994]. At room temperature and pressures above 2 GPa the nonhydrostatic stress in the NaCl pressure medium is saturated, indicating that the stress level has reached the yield point of NaCl [*Weidner et al.*, 1994]. As the sample is embedded in the NaCl medium, the stress field thus determined is assumed to represent the deviatoric stress boundary condition for the sample. Each volume measurement is thus associated with three parameters: pressure, temperature, and nonhydrostatic stress, ( $\sigma_1 - \sigma_3$ ). At room temperature the magnitude of the nonhydrostatic stress can amount to as much as 0.3 GPa (roughly the yield strength of NaCl). We found that the most effective way to minimize nonhydrostatic stress is heating, as the strengths of NaCl and BN decrease dramatically with increasing temperature. Above 600 K, or immediately after cooling from above this temperature, the measured nonhydrostatic stress is generally below 0.05 GPa, which is about the detectability of the current technique. Thus  $P$ - $V$ - $T$  measurements were carried out only during and after heating.

## Results

We obtain volume data for the perovskite along several isotherms at 300, 573, 773, and 973 K, at pressures between 4 and 13 GPa. The procedure is as follows: (1) Compress the starting material at room temperature to the maximum pressure, then heat to 1400 K to completely convert wollastonite into the perovskite structure. (2) Cool from 1400 K to measure both volume and pressure at 973, 773, 573, and 300 K. (3) Lower the ram load at room temperature to the next pressure and repeat heating and cooling at the same temperatures at several pressures. Volume data are collected on cooling only,

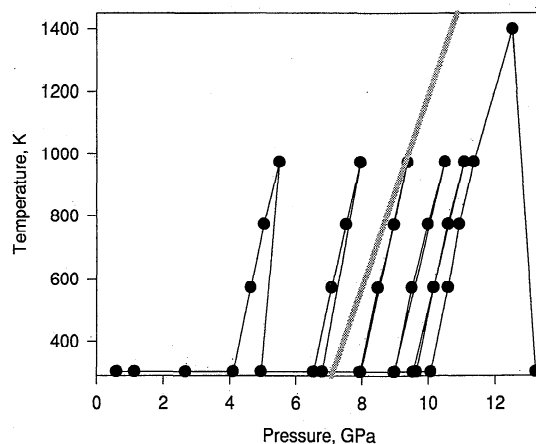


**Figure 3.** Pressure-temperature path of run 13. Each point represents the condition where the unit cell volume of CaSiO<sub>3</sub> perovskite is taken. The heavy gray line represents the phase boundary of CaSiO<sub>3</sub> perovskite determined in situ by *Wang and Weidner* [1994].

in order to minimize nonhydrostatic stresses which may build up during ram load adjustment. The  $P$ - $T$  path is shown in Figure 3. At a constant ram load, pressure changes as temperature is varied, mostly due to thermal pressure effects, as illustrated by Figure 3. About 60% of the data are obtained within the stability field of the perovskite, while 40% are at lower pressures. However, no sign of back transformation of the perovskite structure to a more stable phase is observed above 4 GPa (at any temperature investigated). Amorphization is detected at pressures below 1 GPa (see below). The volume data are summarized in Table 1. Also included in Table 1 are the data obtained by *Wang and Weidner* [1994] between 10 and 13 GPa and up to 1600 K. The whole data set covers a pressure range up to 13 GPa and temperature to 1600 K, with about 80% of the data points within the stability field.

### Amorphization and Anomalous Volume-Pressure Behavior at Low Pressure

It is a well-known observation that CaSiO<sub>3</sub> perovskite is nonquenchable and amorphizes at low pressures [e.g., *Ringwood and Major*, 1971; *Tamai and Yagi*, 1989; *Kanzaki et al.*, 1991; etc.]. However, the effects of the amorphization process on volume have not been addressed previously in connection with equation of state measurements. In a high-temperature X ray diffraction study on (Mg,Fe)SiO<sub>3</sub> perovskite, *Wang et al.* [1994] observed a significant decrease in volume as the perovskite samples were heated at ambient pressure, associated with amorphization of the (Mg,Fe)SiO<sub>3</sub> perovskite. After heating, the samples were found to give a cell volume significantly smaller than the starting value. Following their observations, we established the following criteria of amorphization in CaSiO<sub>3</sub> perovskite: (1) a marked decrease in intensity of the diffraction peaks, (2) a significant increase in background, and (3) a change in the pressure-volume relation associated with criteria 1 and 2.

All three phenomena were observed in CaSiO<sub>3</sub> perovskite at room temperature, as the pressure was lowered from above 1 GPa. Figure 2b shows a diffraction spectrum of the sample obtained at room temperature and 0.59 GPa. A comparison with Figure 2a (11.7 GPa and 1172 K) shows a dramatic drop in diffraction intensity and an increase in the background,

**Table 1.** Summary of the *P-V-T* Data for CaSiO<sub>3</sub> Perovskite Obtained in This Study

Pressure, GPa	Temperature, K	Volume, Å <sup>3</sup>	Δσ, GPa*
<i>Run 13</i>			
12.04	1368	44.76(1)	0.001
11.69	1172	44.54(2)	0.006
11.35	970	44.41(3)	0.007
11.06	977	44.45(2)	-0.018
10.49	980	44.53(3)	0.008
9.37	976	44.71(3)	-0.021
7.95	974	44.92(2)	-0.021
5.51	980	45.44(2)	0.019
10.92	769	44.23(3)	0.018
10.58	769	44.28(2)	0.008
9.98	770	44.38(3)	0.038
8.97	774	44.51(2)	-0.035
7.52	772	44.78(2)	-0.015
5.04	771	45.25(1)	-0.030
10.58	572	44.07(2)	-0.013
10.15	572	44.12(1)	0.023
9.50	575	44.22(2)	0.038
8.48	570	44.37(4)	0.002
7.09	572	44.63(1)	-0.007
4.68	570	45.12(1)	0.011
10.07	306	43.83(2)	-0.017
9.54	303	43.87(3)	-0.004
9.63	304	43.93(3)	-0.004
8.97	302	44.01(3)	0.023
8.98	302	43.99(3)	0.003
7.97	301	44.08(4)	0.031
7.94	303	44.14(2)	-0.001
6.54	303	44.38(4)	-0.006
4.95	301	44.59(4)	0.080
4.15	303	44.87(1)	-0.001
4.12	303	44.87(1)	-0.026
2.66	301	45.03(1)	0.092
1.13†	301	45.39(6)	0.132
0.59‡	301	45.22(4)	0.145
<i>Run 3§</i>			
12.00	1074	44.39(1)	0.000
12.08	1145	44.52(1)	0.047
12.16	1210	44.59(1)	0.051
12.23	1250	44.62(1)	0.062
11.60	1006	44.48(1)	0.118
11.21	904	44.39(1)	0.064
11.07	837	44.35(1)	0.054
10.90	761	44.29(1)	0.071
10.67	672	44.22(1)	0.076
10.46	577	44.15(1)	0.093
12.04	1207	44.60(1)	0.043
12.04	1205	44.60(1)	0.006
11.24	1182	44.73(2)	0.043
10.67	1167	44.81(1)	0.030
10.26	1159	44.88(2)	0.003
<i>Run 4§</i>			
11.61	1177	44.82(1)	0.088
11.85	1261	44.82(1)	0.013
11.77	1339	44.95(2)	-0.022
11.74	1403	45.02(2)	-0.021
11.53	1301	44.90(1)	0.018
11.43	1223	44.82(1)	0.017
11.25	1137	44.76(2)	0.023
11.12	1074	44.68(2)	0.029
10.91	978	44.60(2)	0.011
10.73	894	44.52(1)	0.008
10.51	798	44.46(2)	0.012
11.31	1125	44.73(1)	0.019
<i>Run 5§</i>			
12.16	1128	44.53(2)	0.046
12.25	1318	44.70(1)	0.021
12.23	1381	44.75(1)	0.047

**Table 1.** (continued)

Pressure, GPa	Temperature, K	Volume, Å <sup>3</sup>	Δσ, GPa*
<i>Run 5§ (continued)</i>			
12.01	1469	44.86(1)	0.062
11.69	1594	45.08(5)	0.043

\*Differential stress ( $\sigma_1 - \sigma_3$ ) determined from NaCl peak shifts. Compression is negative.

†Not used in equation of state fit due to high nonhydrostatic stress.

‡Amorphization occurred between 0.6 and 1 GPa.

§Data by Wang and Weidner [1994].

indicative of formation of an amorphous phase. The room temperature volume-pressure behavior is shown in Figure 4a, which also compares our data with the zero-pressure datum measured by Kanzaki *et al.* [1991] on a mostly amorphized sample. A marked decrease in volume is observed as pressure is lowered from 1 GPa to 0.59 GPa. Such an anomalous volume decrease is closely related with the amorphization process, although the detailed mechanism remains to be clarified. Clearly, the effect of amorphization cannot be ignored in equation of state analysis. Including such volume data in the equation of state analysis would result in an overestimate of the bulk modulus.

Durben and Wolf [1992] have studied the amorphization of MgSiO<sub>3</sub> perovskite at elevated temperatures by Raman spectroscopy and found that a temperature of 350 K is sufficient to partially amorphize the perovskite crystals, whose Raman peaks exhibit a residual shift after being cooled back to ambient temperature. The direction of the shift is consistent with a reduced volume.

At this stage the process of amorphization remains unclear. Durben and Wolf [1992] interpret the residual shift as internal stress, since the amorphous material formed after heating is about 30% less dense than the perovskite and must expand. Our X ray data on both perovskites indicate a change in peak shape during amorphization: diffraction peaks of perovskite become broader and may even exhibit some fine features near their shoulder. Thus we are inclined to interpret the amorphization process as creating an increasing number of defects in the formerly perovskite structure. Although it may appear that some "perovskite" peaks can be observed during amorphization, the *P-V-T* relations measured are not representative of the metastable or stable behavior of the perovskite, as volume is no longer a state function. Failure to identify the breakdown of the sample will lead to an incorrect equation of state.

#### Room Temperature Compression and Bulk Modulus

Table 1 lists the measured differential stress for each volume measurement. It can be seen that generally the nonhydrostatic stress is below 0.05 GPa after heating, except for the data below 4 GPa, where no heating was conducted and the nonhydrostatic stress built up gradually on decompression. Especially for the data below 2 GPa, nonhydrostatic stresses are above 0.1 GPa and therefore are discarded in our equation of state fits.

We fit our volume data with the Birch-Murnaghan equations of state

$$P = \frac{3}{2} K_{70} [\eta^{7/3} - \eta^{5/3}] [1 + \frac{3}{4} (K'_{70} - 4)(\eta^{2/3} - 1)], \quad (1)$$

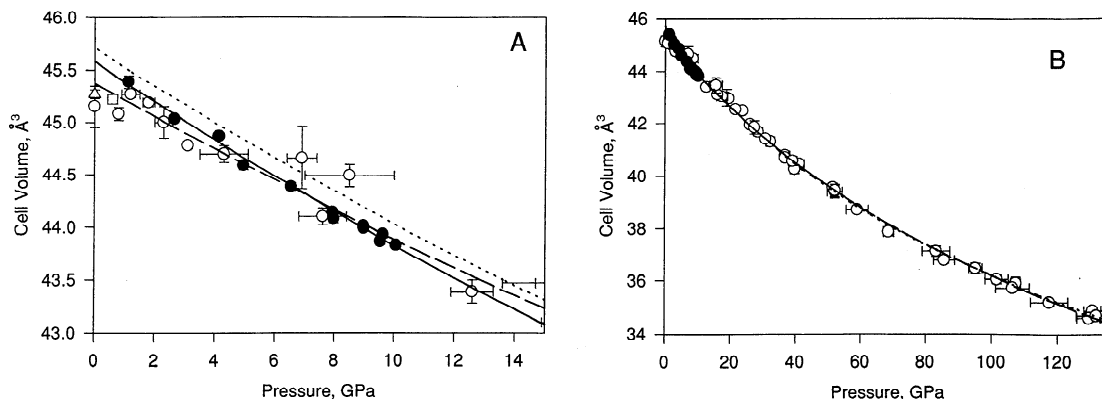


**Figure 4.** Room temperature compression data of CaSiO<sub>3</sub> perovskite obtained in run 13. (a) Unit cell volume of perovskite under stable or metastable conditions (solid circles). Amorphization is observed at pressures below 1 GPa; the measured unit cell volume exhibits a significant decrease as pressure is further lowered (open square). For comparison, the room pressure datum from *Kanzaki et al.* [1991] is shown (open triangle), which was obtained from a partially amorphized sample. Also plotted are the diamond anvil cell data of *Mao et al.* [1989] in a similar pressure range (open circles). Notice that in their data at pressures below 1 GPa, the cell volume also decreases with decreasing pressure. The dashed curve (in both Figure 4a and Figure 4b) is the fit by *Mao et al.* [1989], with  $K_{T0} = 281$  GPa and  $V_0 = 45.37$  Å<sup>3</sup>, with an assumed  $K'_{T0} = 4.0$ . Clearly, the fit deviates from our data. The solid curve is the fit to our data which gives  $K_{T0} = 232$  GPa and  $V_0 = 45.58(4)$  Å<sup>3</sup>, with  $K'_{T0} = 4.8$ . The dotted curve (in both Figure 4a and Figure 4b) is our fit to *Mao et al.*'s data [ $K_{T0} = 244(12)$  GPa and  $V_0 = 45.71(12)$  Å<sup>3</sup>,  $K'_{T0} = 4.8(3)$ ]. (b) Comparison of the room temperature volume with pressure data obtained in this study (solid circles) and previously in the diamond anvil cell up to 134 GPa (open circles [*Mao et al.*, 1989]). The dotted curve is consistent with both data sets.

where  $K_{T0}$  and  $K'_{T0}$  are the ambient isothermal bulk modulus and its pressure derivative, and  $\eta = V_0/V$ . With fixed  $K'_{T0}$  ranging from 3 to 5, the results from fitting equation (1) yield a range of  $K_{T0}$  from 238(7) to 227(7); the corresponding zero-pressure volume ranges from 45.58(4) to 45.60(4) Å<sup>3</sup>, respectively. This narrow range indicates that our  $P$ - $V$  data, which are nonhydrostatic stress free, define a robust trend toward zero pressure.

This range of  $K_{T0}$  value is significantly smaller than the previous values of 275(15) [*Tarrida and Richet*, 1989], 281(4) [*Mao et al.*, 1989], and 325(20) GPa [*Tamai and Yagi*, 1989]. All these previous diamond anvil cell studies were conducted without pressure medium because of the nonquenchable nature of CaSiO<sub>3</sub> perovskite; the level of nonhydrostatic stress is thus unknown. We have found that nonhydrostatic stress can significantly affect the results on  $K_{T0}$ . For example, the room temperature data reported by *Wang and Weidner* [1994] were measured on a CaSiO<sub>3</sub> perovskite sample on decreasing pressure. A careful examination on these data reveals that a differential stress of about 0.2–0.3 GPa built up as pressure was decreased to below 6 GPa; the minimum compressional stress was in the vertical direction, resulting in an underestimate in pressure and therefore an overestimate of the bulk modulus.

In a careful diamond anvil cell study, *Mao et al.* [1989] measured the cell volume of CaSiO<sub>3</sub> perovskite to 134 GPa. Their data are compared with ours in Figures 4a and 4b. Clearly, our data have much smaller uncertainties and define a clearer trend in the  $V$ - $P$  behavior. In the *Mao et al.* study, at pressures greater than 12 GPa the sample was laser heated when the pressure was changed, so that effects of nonhydrostatic stress were minimized. Below 12 GPa, however, laser heating was not applied because of the unstable nature of the material. Thus although the low-pressure data may appear better characterized in terms of pressure uncertainty, nonhydrostatic stress may have been built up, causing the  $P$ - $V$  curve

to change its slope slightly. In addition, as the perovskite structure becomes unstable near zero pressure, amorphization may occur, and as in the observations in our samples, the unit cell volume becomes smaller as pressure is decreased from above 1 GPa. On the basis of a least squares fit of the entire data set to the Birch-Murnaghan equation of state, *Mao et al.* [1989] obtained  $K_{T0} = 281(4)$  GPa with an assumed  $K'_{T0} = 4.0$ . This is the dashed curve shown in Figure 4a. Clearly, this fit is incompatible with our data, as the fit underestimates the unit cell volume below 6 GPa and overestimates it above.

With all of the *Mao et al.* [1989] data weighted by their respective pressure uncertainties (their Table 1), a least squares fit to the Birch-Murnaghan equation of state gives  $K_{T0} = 282(8)$  GPa,  $K'_{T0} = 4.0(2)$ , and  $V_0 = 45.3(5)$  Å<sup>3</sup>. When the lower-volume data below 1 GPa (most likely contaminated by amorphization) are excluded, the fit using equation (1) yields  $K_{T0} = 268(8)$  GPa,  $K'_{T0} = 4.3(2)$ , and  $V_0 = 45.47(6)$  Å<sup>3</sup>, with the same weighting scheme. This latter  $K_{T0}$  is significantly smaller than the fitting result based on the entire data set. This is not surprising, as  $K_{T0}$  corresponds to the slope of the  $P$ - $V$  curve at zero pressure.

Although the data of *Mao et al.* [1989] below 12 GPa appear to have smaller pressure uncertainties, they are most likely contaminated by nonhydrostatic stress and thus should not be weighted more than the higher-pressure data, which have been laser heated. If we weight the remaining data equally, this leads to  $K_{T0} = 244(12)$  GPa,  $K'_{T0} = 4.8(3)$ , and  $V_0 = 45.71(12)$  Å<sup>3</sup>. This is the dotted curve in Figure 4a. In Figure 4b we compare this fit with that of *Mao et al.* [1989] over the entire pressure range. At pressures above 15 GPa the two fits are virtually identical; at lower pressures the latter fit is more consistent with the slope defined by our data (Figure 4a). These latter equation of state parameters describe the measurements from both the diamond anvil cell and the more accurate large-volume press data. This analysis indicates that

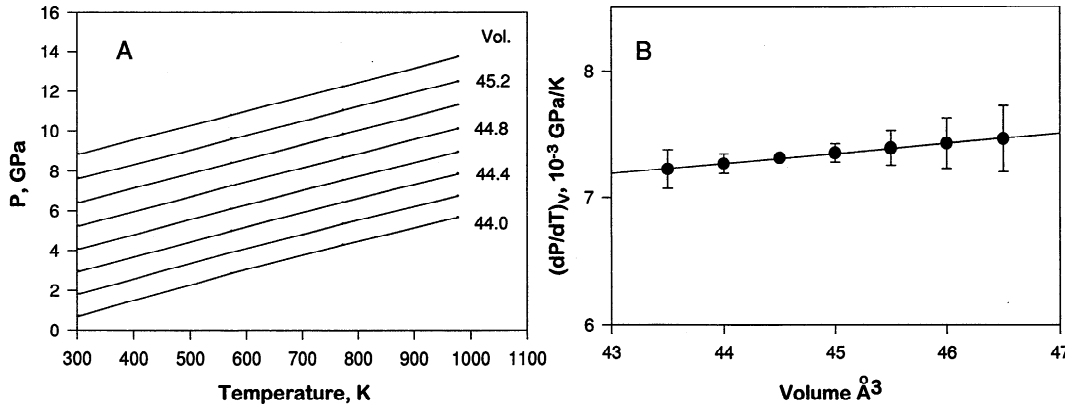


**Figure 5.** Isochoric data of CaSiO<sub>3</sub> perovskite interpolated within the pressure and temperature range of the measurement. (a) Isochores in the  $P$ - $T$  space showing a nearly linear relation between pressure and temperature for each constant unit cell volume. (b) Slope of the isochores in Figure 5a as a function of unit cell volume. A linear fit to the data gives  $(\partial K_T/\partial T)_V = -0.36(8) \times 10^{-2} \text{ GPa K}^{-1}$ .

high-precision data on the low-pressure side of the  $P$ - $V$  measurements are critical in constraining  $K_{T0}$  and that a combination with high-pressure data helps to constrain  $K'_{T0}$ . Unfortunately, there is a small but noticeable systematic shift in volumes between our data and those of *Mao et al.* [1989] (see Figure 4), preventing us from incorporating the two data sets in the equation of state fit. We thus adopt  $K'_{T0} = 4.8$  from the above analysis on *Mao et al.* data in fitting our data with equation (1) to obtain  $K_{T0} = 232(8) \text{ GPa}$  and  $V_0 = 45.58(4) \text{ \AA}^3$  for our data (the solid curve in Figure 4a).

### Thermal Equation of State Analysis

**Isochoric and isobaric interpolation.** We interpolate the volume data within the pressure and temperature range of the measurements to obtain isochoric data  $(\partial P/\partial T)_V$ . At each volume, pressure is linear with temperature (Figure 5a), and the slope represents  $(\partial P/\partial T)_V$ . In Figure 5b the  $(\partial P/\partial T)_V$  values are plotted against the unit cell volume and again show linear variations within the experimental resolution. The slope of the  $(\partial P/\partial T)_V$  versus  $V$  plot is  $7.9(2) \times 10^{-5} \text{ GPa K}^{-1}$ . According to the thermodynamic identity  $(\partial P/\partial T)_V = \alpha K_T$ , the slope in Figure 5b is  $\partial(\alpha K_T)/\partial V$ . In addition,  $\alpha_0 K_{T0}$  can be measured directly from the curve at  $V = V_0 = 45.58 \text{ \AA}^3$  to be  $7.2 \times 10^{-3} \text{ GPa K}^{-1}$ . As no temperature dependence is detected in the pressure and temperature range of the data, we assume that the slope is approximately  $[\partial(\alpha K_T)/\partial V]_T$ , which is equal to  $-(\partial K_T/\partial T)_V/V$ . Therefore at zero pressure, we have  $(\partial K_T/\partial T)_V = -0.36 \times 10^{-2} \text{ GPa K}^{-1}$ . From the thermodynamic identity

$$(\partial K_T/\partial T)_V = (\partial K_T/\partial T)_P + \alpha_0 K_{T0} (\partial K_T/\partial P)_T \quad (2)$$

we obtain  $(\partial K_T/\partial T)_P = -0.031 \text{ GPa K}^{-1}$ , with  $\alpha_0 K_{T0} = 7.2 \times 10^{-3} \text{ GPa K}^{-1}$ ,  $V_0 = 45.58 \text{ \AA}^3$ , and  $(\partial K_T/\partial P)_T = 4.8$ . For  $K_{T0} = 232 \text{ GPa}$ ,  $\alpha_0$  is about  $3.1 \times 10^{-5} \text{ K}^{-1}$ . We also note that fitting  $(\partial P/\partial T)_V$  as a linear function of  $\ln V$  yields very similar results.

We then interpolate the data to obtain volumes as a function of temperature at constant pressure. These isobaric data give thermal expansion directly at each pressure, where the logarithm of volume is then fitted by a linear function in temperature. Attempts have been made to fit these isobaric data to obtain the temperature dependence of thermal expansion. In all cases, however, even with a linear term in the thermal

expansion, i.e.,  $\alpha = a + bT$ , the coefficient  $b$  is found very small (of the order of  $10^{-11} \text{ K}^{-2}$ ), with an uncertainty several orders of magnitude greater than the value itself (about  $10^{-9}$ ). Thus we conclude that at each pressure, the thermal expansion coefficient is best expressed as a constant, independent of temperature within of experimental conditions and the uncertainties. Of course, as temperature is decreased to close to 0 K, thermal expansion is expected to vanish; our data do not provide any constraint toward this end.

*Wang and Weidner* [1994] observed that the thermal expansion coefficient of CaSiO<sub>3</sub> perovskite is also independent of temperature within the stability field (10–12 GPa) up to 1600 K. A similar behavior was also observed in MgSiO<sub>3</sub> perovskite by *Wang et al.* [1994], *Utsumi et al.* [1995], and *Funamori et al.* [1995]. These studies show that under pressure the thermal expansion coefficient is essentially constant over a wide range of temperatures up to about 1800 K at pressures from 4 to 30 GPa. Thus it appears that pressure suppresses the temperature dependence of thermal expansion in both MgSiO<sub>3</sub> and CaSiO<sub>3</sub> perovskite, making the thermal expansion coefficient virtually independent of temperature from 300 to well above 1000 K.

The isobaric thermal expansion data are plotted in Figure 6 to illustrate the pressure dependence in  $\alpha$ . The *Wang and Weidner* [1994] data are also included in Figure 6 for comparison. The isobaric thermal expansion data obtained from several runs agree very well. A linear fit to all of the thermal expansion data yields  $(\partial\alpha/\partial P)_T = -5.24(19) \times 10^{-7} \text{ GPa}^{-1} \text{ K}^{-1}$ , with  $\alpha_0 = 3.23(2) \times 10^{-5} \text{ K}^{-1}$ . From thermodynamic identity  $(\partial\alpha/\partial P)_T = (\partial K_T/\partial T)_P K_T^{-2}$ , we obtain  $(\partial K_T/\partial T)_P = -0.028 \text{ GPa K}^{-1}$  at ambient condition.

**Thermal pressure equation of state.** O. L. Anderson [Anderson, 1980, 1984; Anderson et al., 1989] proposed a thermal equation of state based on the Mie-Grüneisen theory, by computing thermal pressures from thermodynamic parameters measurable in the laboratory. At any temperature  $T$  and for a given volume  $V$ , the pressure can be expressed as the sum of the static pressure at a reference temperature  $T_0$  and the thermal pressure  $\Delta P_{\text{th}}$  [e.g., *Jackson and Rigden*, 1996].

$$P(V, T) = P(V, T_0) + \Delta P_{\text{th}} = \sum b_i X_i(\eta, T) \quad (3a)$$

where

$$X_1 = \eta^{7/3} - \eta^{5/3} \quad b_1 = 3K_T(V_0, T_0)/2$$

$$X_2 = X_1(\eta^{2/3} - 1) \quad b_2 = \frac{9}{8}K_T(V_0, T_0)[K'_{T0}(V_0, T_0) - 4]$$

$$P(V, T_0) = b_1X_1 + b_2X_2 \quad (3b)$$

$$X_3 = (T - T_0), \quad b_3 = \alpha K_T$$

$$X_4 = -(T - T_0) \ln \eta \quad b_4 = (\partial K_T / \partial T)_V$$

$$X_5 = (T - T_0)^2 \quad b_5 = [(\partial^2 P / \partial T^2)_V] / 2$$

From these coefficients some relevant thermoelastic parameters can be calculated, for example [see *Jackson and Rigden, 1996*],

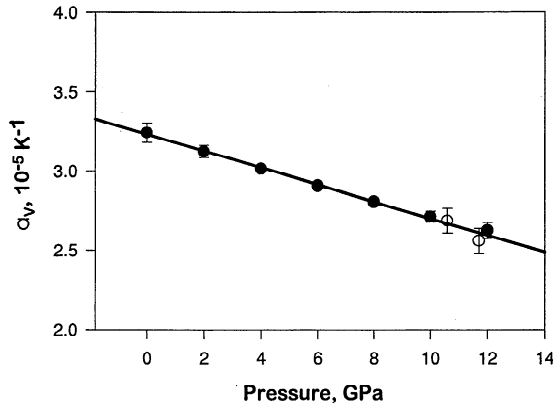
$$(\partial K_T(V, T) / \partial T)_P = (\partial K_T(V, T) / \partial T)_V - \alpha K_T(V, T) K'_T(V, T)$$

$$(\partial \alpha / \partial T)_V = (\partial^2 P / \partial T^2)_V / K_T(V, T) - (\partial P / \partial T)_V (\partial K_T / \partial T)_V / K_T^2(V, T) \quad (3c)$$

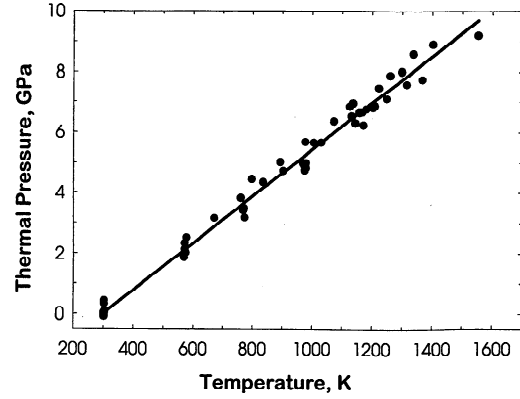
$$(\partial \alpha / \partial T)_P = (\partial \alpha / \partial T)_V - \alpha (\partial K_T / \partial T)_P / K_T(V, T)$$

Figure 7 shows our data obtained in all four runs, in the form of thermal pressure, which is the difference between the measured pressure and the calculated pressure based on the room temperature ( $T_0 = 300$  K) Birch-Murnaghan equation of state at the same volume. It is clear that the data fall in a narrow trend, varying linearly with temperature. A fit using (3a) with the first three terms (but with a fixed  $K'_{T0} = 4.8$ ) yields  $V_0 = 45.61(4) \text{ \AA}^3$ ,  $K_{T0} = 231(7)$  GPa, and  $\alpha_0 = 3.33(6) \times 10^{-5} \text{ K}^{-1}$ . When the fourth term is included,  $b_4$  is found to be  $-5.27 \times 10^{-3} \text{ GPa K}^{-1}$ , but the uncertainty is 0.02 GPa  $\text{K}^{-1}$ ; clearly,  $b_4$  cannot be resolved from this fit. If we fix  $b_4$  at  $-3.6 \times 10^{-3} \text{ GPa K}^{-1}$ , according to the isochoric results, then we obtain  $V_0 = 45.61(4) \text{ \AA}^3$ ,  $K_{T0} = 230(7)$  GPa, and  $\alpha_0 = 3.20(6) \times 10^{-5} \text{ K}^{-1}$ . Results from various fits are summarized in Table 2.

To examine the effects of systematic errors in the four runs, we have analyzed the data from run 13 alone. A similar weighted fit using the first three terms in (3a) gives  $V_0 = 45.61(2) \text{ \AA}^3$ ,  $K_{T0} = 229(4)$  GPa, and  $\alpha_0 = 3.04(5) \times 10^{-5} \text{ K}^{-1}$ . Again,  $b_4$  cannot be resolved; fixing  $b_4$  at  $-3.6 \times 10^{-3} \text{ GPa K}^{-1}$  yields  $V_0 = 45.61(2) \text{ \AA}^3$ ,  $K_{T0} = 227(4)$  GPa, and



**Figure 6.** Isobaric thermal expansion obtained as a function of pressure. Solid circles are obtained by fitting the interpolated cell volumes (e.g., Figure 5a). The slope of this plot gives a  $\partial \alpha / \partial P$  of  $-5.24(19) \times 10^{-7} \text{ GPa}^{-1} \text{ K}^{-1}$ . Open circles are the isobaric thermal expansion data obtained by *Wang and Weidner [1994]*, agreeing well with the present measurement.



**Figure 7.** Thermal pressure of CaSiO<sub>3</sub> perovskite up to 13 GPa and 1600 K. All of the data listed in Table 1 are used.

$\alpha_0 = 3.04(5) \times 10^{-5} \text{ K}^{-1}$ . The similarity in the values indicates that the results are quite robust.

The fact that  $(\partial K_T / \partial T)_V$  is virtually nonresolvable from zero suggests that there is no volume dependence in thermal pressure. Indeed, when the thermal pressure is plotted against volume (Figure 8), measurements along all the isotherms are best fit by a constant thermal pressure line. Taking  $(\partial K_T / \partial T)_V = 0$ , equation (2) gives  $(\partial K_T / \partial T)_P = -0.035 \text{ GPa}^{-1} \text{ K}^{-1}$ , for  $K_{T0} = 232$  GPa,  $\alpha_0 = 3.2 \times 10^{-5} \text{ K}^{-1}$ , and  $K'_{T0} = 4.8$ .

As an interesting outcome from Figure 8, the thermal pressure being independent of volume indicates that  $[\partial(\alpha K_T) / \partial T]_T = (\delta_T - K_T) \alpha K_T / V = 0$  [*Anderson et al., 1992*]. Thus the Anderson-Grüneisen parameter  $\delta_T = -(\partial K_T / \partial T)_P / \alpha K_T = K'_T = 4.8$ .

#### High-temperature Birch-Murnaghan equation of state.

We now assume that the Birch-Murnaghan equation of state can be applied to any given temperature and try to analyze the whole data set with such an equation of state. We use equation (1), with  $\eta = V_R / V$ ; now  $K_{T0}$ ,  $V_R$ , and  $K'_{T0}$  are parameters at zero pressure and at any constant temperature  $T$ ;  $K'_{T0}$  is again assumed constant ( $= 4.8$ ).  $V_R = V(0, T)$  is related to  $V_0$  via zero-pressure thermal expansion  $\alpha(0, T)$ , which is expressed as  $a + bT - cT^2$ , where  $a$ ,  $b$ , and  $c$  are all positive constants.

It turns out that the results of the fit using this equation of state vary noticeably with various weighting functions used, when both  $K_{T0}$  and  $V_0$  are set free in the fit. A close correlation is observed in these fits: where  $K_{T0}$  is low,  $V_0$  is high and  $|(\partial K_T / \partial T)_P|$  is low, and vice versa. Thus we are forced to fix  $K_{T0}$  as well as  $V_0$ , at 232 GPa and 45.58  $\text{ \AA}^3$ , respectively. Even in this situation, the coefficients  $b$  and  $c$  in the zero-pressure thermal expansion still cannot be resolved in the weighted fits. The coefficient  $b$  is barely resolvable in an unweighted fit (Table 2). With both  $b$  and  $c$  set to zero, the unweighted fit gives  $(\partial K_T / \partial T)_P = -0.022(10) \text{ GPa K}^{-1}$ , and  $\alpha_0 = 3.06(14) \times 10^{-5} \text{ K}^{-1}$  (shown in Figure 9).

**Summary of the equation of state analysis.** Table 2 gives the thermoelastic properties of CaSiO<sub>3</sub> perovskite using various approaches. For each parameter the uncertainties in parentheses represent the standard deviation obtained from the fit. Other parameters may be derived from equations such as (3c); for these parameters we do not give uncertainties in the table, as they can be obtained by standard error propagation. We prefer the parameter set obtained from the thermal pressure equation of state fit with a weighting function  $1/\Delta P^2(P) + 1/\Delta P^2(V)$ , where  $\Delta P(P) = 2|\sigma_1 - \sigma_3|$  is the pressure

**Table 2.** Summary of Thermoelastic Parameters for CaSiO<sub>3</sub> Perovskite Obtained From Various Approaches

Parameter	Isothermal Room Temperature	Thermal Pressure Equation of State					High-Temperature Birch-Murnaghan		
		Isobaric	Isochoric	Weighted, 1	Weighted, 2	Unweighted	Weighted	Unweighted, 1	Unweighted, 2
$K_{T0}$ , GPa	232(8)	...	...	233(7)	229(4)	233(9)	[232]	[232]	[232]
$K'_{T0}$	[4.8]	[4.8]	[4.8]	[4.8]	[4.8]	[4.8]	[4.8]	[4.8]	[4.8]
$V_0$ , Å <sup>3</sup>	45.58(4)	...	...	45.60(5)	45.61(2)	45.58(4)	[45.58]	[45.58]	[45.58]
$\alpha_0$ , 10 <sup>-5</sup> K <sup>-1</sup>	...	3.23(2)	3.1	3.23	3.01	3.06	3.55(18)	3.06(14)	3.19(48)
$(\partial P/\partial T)_{V_0}$ , 10 <sup>-3</sup> GPa K <sup>-1</sup>	...	7.2	7.2(3)	7.5(5)	6.9(1)	7.1(1)	8.2	7.1	7.4
$(\partial K_T/\partial T)_{V_0}$ , GPa K <sup>-1</sup>	...	0.008	-0.004	0.005(22)	[0]	[0]	0.004	0.012	0.001
$(\partial K_T/\partial T)_P$ , GPa K <sup>-1</sup>	...	-0.028	-0.031	-0.031	-0.033	-0.034	-0.036(8)	-0.022(10)	-0.035(15)
$(\partial \alpha/\partial P)_T$ , 10 <sup>-7</sup> (GPa K) <sup>-1</sup>	...	-5.24(19)	-5.8	-5.7	-6.3	-6.4	-6.7	-4.1	-6.5
$(\partial \alpha/\partial T)_P$ , 10 <sup>-8</sup> K <sup>-2</sup>	...	[0]	...	0.36	0.43	0.44	[0]	[0]	0.45(40)
$(\partial^2 P/\partial T^2)_{V_0}$ , GPa <sup>2</sup> K <sup>-2</sup>	...	...	...	[0]	[0]	[0]	[0]	[0]	[0]

Square brackets indicate fixed parameters in the fit. Uncertainties given in parentheses represent the standard deviation obtained from the fit.

uncertainty due to deviatoric stress and  $\Delta P(V) = K_{T0} \Delta V/V$  is the pressure uncertainty due to volume error  $\Delta V$ . The preferred values,  $(\partial K_T/\partial T)_P = -0.033$  GPa K<sup>-1</sup> and  $\alpha_0 = 3.06 \times 10^{-5}$  K<sup>-1</sup>, give an Anderson-Grüneisen parameter  $\delta_T = 4.65$ , which is about equal to  $K'_T = 4.8(3)$ .

## Discussion

### Comparison of Thermoelastic Behavior Between CaSiO<sub>3</sub> and MgSiO<sub>3</sub> Perovskites

Weidner and Zhao [1992] have proposed a formalism in defining the equation of state of perovskite which allows evaluation of the effects of structural distortions. Assuming that the SiO<sub>6</sub> octahedra are regular, the unit cell volume of the orthorhombic perovskite may be written as

$$V = abc = V_0 \cos^2 \Phi, \quad (4)$$

where  $\Phi$  is the tilt angle about the “threefold” axes of the octahedra which describes the degree of distortion of the perovskite structure and  $V_0$  is the volume of an idealized cubic perovskite that depends only on the octahedron bond length [Si-O]:

$$V_0 = (2[\text{Si-O}])^3 Z, \quad (5)$$

where  $Z$  is the number of chemical formulae per unit cell. The tilt angle for the orthorhombic MgSiO<sub>3</sub> perovskite ( $Pbnm$ ) can be estimated from unit cell dimensions via

$$\Phi = \cos^{-1} (\sqrt{2} a^2/bc). \quad (6)$$

Thus pressure- and temperature-induced volume change may be expressed as a combination of changes in bond length and tilt angle. For thermal expansion ( $\alpha$ ) and compressibility ( $\beta$ ), differentiating (4) with respect to temperature and pressure leads to

$$\alpha_V = \alpha_{V_0} + \alpha_{V_\Phi} = 3 \partial \ln [\text{Si-O}]/\partial T + 2 \partial \ln \cos \Phi/\partial T \quad (7)$$

$$\beta_V = \beta_{V_0} + \beta_{V_\Phi} = -3 \partial \ln [\text{Si-O}]/\partial P - 2 \partial \ln \cos \Phi/\partial P. \quad (8)$$

It has been recognized that the tilt angle and bond length calculated using (4)–(6) show a systematic offset compared with those derived from atomic positions determined from structural analysis. For example, in MgSiO<sub>3</sub> perovskite, the ambient [Si-O] bond length (1.778 Å) is underestimated by

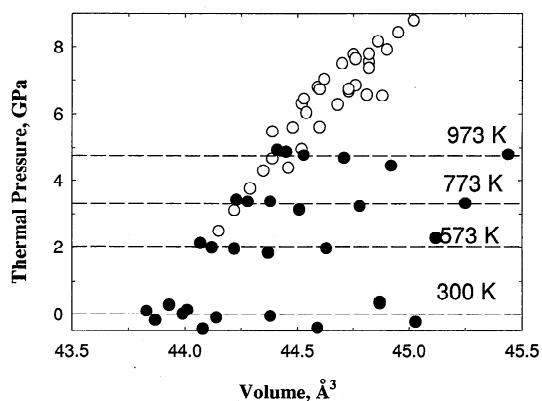


**Figure 8.** Thermal pressure as a function of volume. Solid circles indicate data from run 13. Within the experimental errors, no volume dependence in thermal pressure is observed.

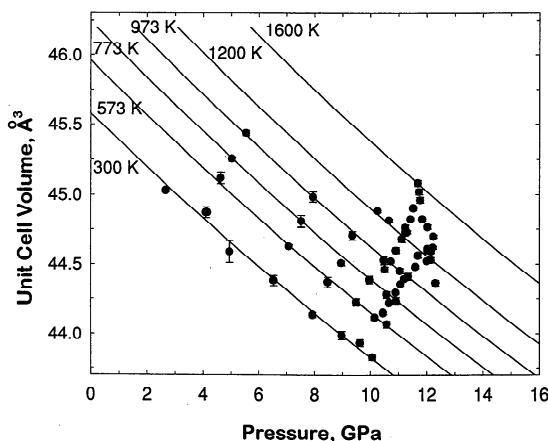


**Figure 9.** High-temperature Birch-Murnaghan equation of state fit (unweighted fit 1 in Table 2) to all CaSiO<sub>3</sub> perovskite data listed in Table 1.

0.015 Å (~1%), compared with the single-crystal X ray data (1.793 Å [Horiuchi *et al.*, 1987]). A similar situation is observed for neighborite, NaMgF<sub>3</sub> [Zhao *et al.*, 1993, 1994] and is attributed to slight distortion in the octahedra. The pressure and temperature dependence (i.e., the partial derivatives in (7) and (8)), however, is rather consistent with structural data [Zhao *et al.*, 1993]. In case of CaSiO<sub>3</sub>, insofar as the structure is cubic ( $Z = 1$ ), the tilt angle must be zero, and the volume is directly related with [Si-O] bond distance via equation (5). Table 3 compares selected structural and thermoelastic parameters in response to pressure and temperature for the two perovskites.

Figures 10 and 11 show the bond length and tilt angle of MgSiO<sub>3</sub> perovskite as a function of pressure and temperature, respectively, from the data reported by Wang *et al.* [1994]. In the pressure plot (Figure 10), average linear thermal expansion coefficients have been used to correct the data to room temperature. These linear thermal expansion data are obtained from fitting the individual cell edge data in separate runs in Table 4 of Wang *et al.* [1994]. In the temperature plot (Figure 11), the cell parameters are corrected to zero pressure using the linear compressibility data of Mao *et al.* [1991] obtained at room temperature up to 30 GPa ( $\beta_a = 1.29$ ,  $\beta_b = 1.05$ , and  $\beta_c = 1.33$  TPa<sup>-1</sup>). Superimposed on the bond length data are the [Si-O] length of CaSiO<sub>3</sub> perovskite measured in the present study. Similar to the MgSiO<sub>3</sub> perovskite, the bond length [Si-O], defined as  $a/2$  for CaSiO<sub>3</sub>, is also corrected using a linear compressibility ( $\beta_a = 1/3K_{T0}$ ) in Figure 10 and an average linear thermal expansion of  $\alpha_a = \alpha_V/3$  in Figure 11.

During compression the tilt angle for MgSiO<sub>3</sub> increases ( $\partial\Phi/\partial P = 2.72 \times 10^{-2}$  deg GPa<sup>-1</sup>), whereas the bond length decreases ( $\partial[\text{Si-O}]/\partial P = -1.979 \times 10^{-3}$  Å GPa<sup>-1</sup>) (Figure 10). The contributions to the compressibility are different by one order of magnitude, with  $\beta_{V_0} = 3.3 \times 10^{-3}$  GPa<sup>-1</sup> and  $\beta_{V_\Phi} = 3.2 \times 10^{-4}$  GPa<sup>-1</sup>, respectively. On the other hand, the magnitude of the change in bond length is very similar to that of CaSiO<sub>3</sub>, where  $\partial[\text{Si-O}]/\partial P = -2.107 \times 10^{-3}$  Å GPa<sup>-1</sup> and  $\beta_{V_0} = 3.6 \times 10^{-3}$  GPa<sup>-1</sup>. The similarity in compressibilities of both perovskites indicates that the compression mechanism of MgSiO<sub>3</sub> is similar to that of CaSiO<sub>3</sub>. Thus compression of MgSiO<sub>3</sub> is overwhelmingly dominated by change in the [Si-O] bond distance.

However, it is evident from Figure 11 that upon heating MgSiO<sub>3</sub> perovskite expands both by changing bond length and by adjusting the tilt angle. The change in the tilt angle is about  $-7.563 \times 10^{-4}$  deg K<sup>-1</sup>, corresponding to a mean  $\alpha_{V_\Phi}$  of  $0.88 \times 10^{-5}$  K<sup>-1</sup>, over the entire temperature range of 300 to 1300 K. The mean slope of the bond distance change is  $7.81 \times 10^{-5}$

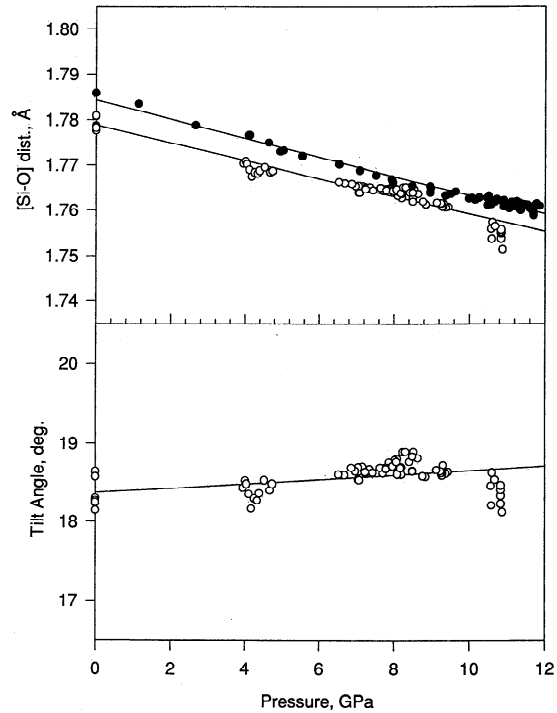


**Figure 10.** Calculated [Si-O] bond length and tilt angle of MgSiO<sub>3</sub> perovskite as a function of pressure, based on data of Wang *et al.* [1994] to 11 GPa and 1300 K (open circles). [Si-O] distance is also calculated from the cell edge length  $a$  of CaSiO<sub>3</sub> perovskite for comparison (solid circles). Linear thermal expansion coefficients, obtained from fitting the cell edge data of Wang *et al.* [1994] are used to correct the data to 300 K. For CaSiO<sub>3</sub>, a linear thermal expansion of  $\alpha_V/3$  is used for the correction. Note that [Si-O] bond distances in both materials respond similarly to pressure, but for MgSiO<sub>3</sub> the tilt angle changes very little. The total volume compression is dominated by shrinking in bond length.

Å K<sup>-1</sup>, which gives an average  $\alpha_{V_0}$  about  $1.32 \times 10^{-5}$  K<sup>-1</sup>. This value is less than half of the bond length expansion ( $1.833 \times 10^{-5}$  Å K<sup>-1</sup>) for CaSiO<sub>3</sub> (Figure 11). Clearly, the [Si-O] bond distance responds to heating quite differently in the two perovskites.

Thus in MgSiO<sub>3</sub> orthorhombic perovskite the mechanisms of thermal expansion and compression are quite distinct, with the former dominated by change in the tilt angle and the latter dominated by change in [Si-O] bond distance. Therefore if pressure and temperature are increased in such a way as to maintain a constant volume, both the octahedron size and the tilt angle will be reduced. For each constant volume the various degrees of the changes in bond length and tilt angle will depend on the pressure and temperature conditions. From this, one can directly infer that frequencies ( $\nu$ ) of at least some of the normal modes of vibration will show a strong intrinsic temperature dependence, that is,  $(\partial\nu/\partial T)_V$  different from 0. Such a behavior is characteristic of intrinsic anharmonicity [e.g., Mammone and Sharma, 1979; Gillet *et al.*, 1991], and mantle perovskite might be a strongly anharmonic material. In describing the  $P$ - $V$ - $T$  behavior of materials, one of the most commonly used assumptions is that phonon eigenfrequencies depend only on volume, which expresses the net effect of the pressure and temperature state of the material. In view of the distinctive pressure and temperature effects on the structure of

**Table 3.** Some Structural Parameters of MgSiO<sub>3</sub> and CaSiO<sub>3</sub> Perovskites in Responding to Pressure and Temperature

	MgSiO <sub>3</sub>	CaSiO <sub>3</sub>
Si-O Distance, * Å	1.780 (1.793)†	1.786
$\Phi^*$ , deg	18.2	0.0
$\beta_{V_0}$ , TPa <sup>-1</sup>	3.3	3.5
$\beta_{V_\Phi}$ , TPa <sup>-1</sup>	3.2	0.0
$\alpha_{V_0}$ , 10 <sup>-5</sup> K <sup>-1</sup>	1.32	3.08
$\alpha_{V_\Phi}$ , 10 <sup>-5</sup> K <sup>-1</sup>	0.88	0.0

\*Calculated from equations (5) and (6).

†Datum in parentheses is from single-crystal structural refinement [Horiuchi *et al.*, 1987].

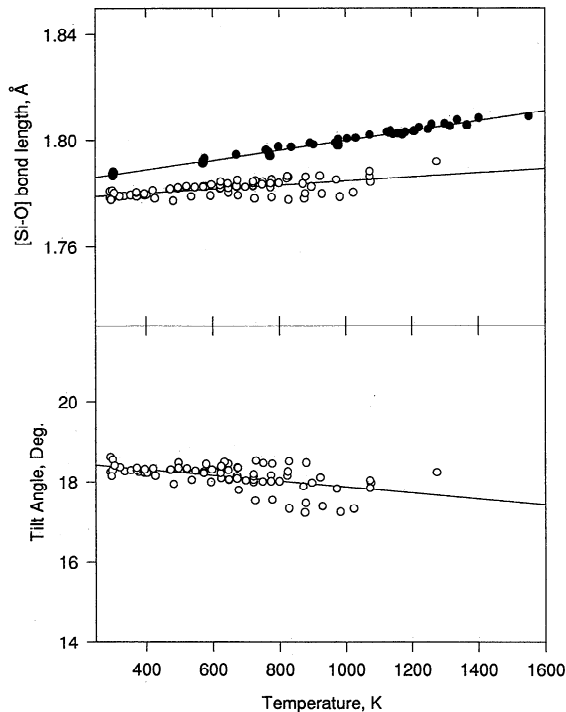


**Figure 11.** Calculated [Si-O] bond distance and tilt angle of MgSiO<sub>3</sub> perovskite using equations (6)–(8) as a function of temperature, based on data of Wang *et al.* [1994] to 11 GPa and 1300 K (open circles). [Si-O] distance is also calculated from the cell edge length  $a$  of CaSiO<sub>3</sub> perovskite for comparison (solid circles). Note that the slope  $\partial[\text{Si-O}]/\partial T$  for CaSiO<sub>3</sub> is about 2 times that for MgSiO<sub>3</sub>. Roughly about 30% of the volume expansion of MgSiO<sub>3</sub> is due to [Si-O] bond increase with temperature; the dominant change in volume is due to change in tilt angle.

MgSiO<sub>3</sub> perovskite, however, this simple picture may be invalid.

#### Implications for Lower Mantle Composition Models

The new data on CaSiO<sub>3</sub> perovskite allow us to examine the effects of this material on constraints on composition of the lower mantle. Table 4 lists thermoelastic parameters of CaSiO<sub>3</sub> perovskite used for this analysis. In extrapolating the thermal equation of state to lower mantle conditions, we assume that

**Table 4.** Thermoelastic Parameters for MgSiO<sub>3</sub> and CaSiO<sub>3</sub> Perovskites

	MgSiO <sub>3</sub> *	CaSiO <sub>3</sub>
$V_0$ , cm <sup>3</sup> mol <sup>-1</sup>	24.46	27.45
$\rho_0$ , g cm <sup>-3</sup>	4.108	4.231
$\alpha_0$ , 10 <sup>-5</sup> K <sup>-1</sup>	1.7	3.01
$K_{T0}$ , GPa	261	232
$K'_{T0}$	4	4.8
$(\partial K_T/\partial T)_p$ , GPa/K	-0.023	-0.033
$\Theta_D$ , K	1030	1100†
$\delta_{T0}$	4.9	4.8
$\gamma_0$	1.4	1.7‡
$q$ ‡	1	1

\*Data from Wang *et al.* [1994].

†From Wang and Weidner [1994].

‡Assumed pressure dependence in Gruneisen parameter through volume.

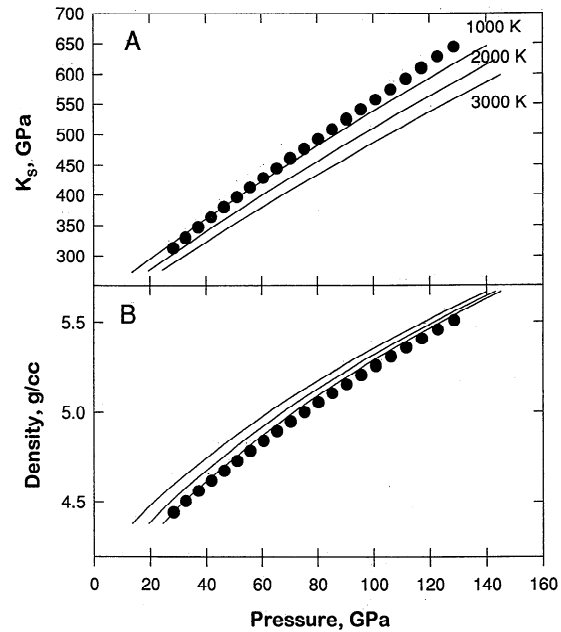


**Figure 12.** Thermoelastic parameters of CaSiO<sub>3</sub> perovskite (solid curves) extrapolated to lower mantle conditions as compared with PREM (solid symbols). (a) Adiabatic bulk modulus. Data for CaSiO<sub>3</sub> are plotted along several adiabats with the foot temperatures of 1000, 2000, and 3000 K. (b) Similar plot for density. Density of CaSiO<sub>3</sub> perovskite is slightly higher than that of PREM.

the ambient Anderson-Gruneisen parameter ( $\delta_{T0} = 4.8$ ) is applicable for the pressure and temperature conditions of the lower mantle. Thermal expansion at any pressure is thus approximated by  $\alpha = \alpha_0(V/V_0)^{\delta_T}$ . The Gruneisen parameter is estimated by Wang and Weidner [1994] from the fitting results at 10–12 GPa ( $\gamma = 1.60 - 1.75$ ), with  $\gamma/\gamma_0 = (V/V_0)^q$ . For  $q = 1$ , the estimated  $\gamma_0$  ranges from 1.66 to 1.82 [Wang and Weidner, 1994].

With these thermoelastic parameters we calculate the density and  $K_s$  for CaSiO<sub>3</sub> perovskite in the lower mantle. Figure 12a shows the adiabatic bulk modulus of the perovskite along three adiabats 1000, 2000, and 3000 K (the foot temperatures are at zero pressure), in comparison with the preliminary reference Earth model (PREM) [Dziewonski and Anderson, 1981]. Along the 2000 K adiabat, the  $K_s$  of the perovskite is very close to that of PREM at the top of the lower mantle but gradually deviates. Near the core-mantle boundary the bulk modulus is about 10% lower than that of PREM. Given that CaSiO<sub>3</sub> perovskite is most likely below 10 vol % in the lower mantle, such a difference in  $K_s$  would be insignificant in affecting previous analyses of composition based on data on (Mg,Fe)SiO<sub>3</sub> perovskite and magnesiowüstite alone.

Figure 12b shows density profiles of CaSiO<sub>3</sub> perovskite along same adiabats. Comparing with PREM, CaSiO<sub>3</sub> may be slightly denser, but only by about 1%. Thus we conclude that in modeling the composition of the lower mantle, CaSiO<sub>3</sub> perovskite can be regarded as invisible.

However, the bulk modulus of CaSiO<sub>3</sub> perovskite is significantly higher than that of the Transition Zone. As this perovskite may begin to form at pressures as low as 17 GPa [Gasparik, 1989, 1990], it will contribute to the velocity gradients in this region of the Earth.

## Conclusions

Using synchrotron X radiation and a DIA-type, cubic anvil apparatus,  $P$ - $V$ - $T$  measurements on  $\text{CaSiO}_3$  have been carried out at pressures between 0 and 13 GPa and temperatures up to 1600 K, under quasi-hydrostatic conditions with nonhydrostatic stresses carefully determined. At room temperature, amorphization is observed at pressures below 1 GPa. Although some of the "perovskite" diffraction lines seem to remain at these low pressures, the unit cell volume exhibits a significant decrease compared with high-pressure volumes. This behavior is compared with that of  $\text{MgSiO}_3$  perovskite, where on heating to above 400 K at zero pressure, a similar amorphization process has been observed [Wang et al., 1994]. Once amorphization occurs, volume is no longer a state function and cannot be used in determining equation of state parameters.

A complete thermal equation of state has been determined for  $\text{CaSiO}_3$  perovskite. The data were analyzed in various ways, and the results are consistent. We have identified a set of thermoelastic parameters that are compatible with both our data to 1600 K and previous diamond anvil cell measurements at room temperature to 134 GPa. The ambient isothermal bulk modulus is 232(8) GPa, with  $K'_{T0} = 4.8(3)$  and  $V_0 = 45.58(4) \text{ \AA}^3$ . The observed  $P$ - $V$ - $T$  behavior of the cubic  $\text{CaSiO}_3$  perovskite is compared with that of the orthorhombic perovskite  $\text{MgSiO}_3$  to show that crystal structure plays an important role in equations of state. For  $\text{MgSiO}_3$ , as Si-O-Si tilt angle and [Si-O] bond distance respond to pressure and temperature rather differently, care must be taken in extrapolating the laboratory-measured  $P$ - $V$ - $T$  relations to deep mantle conditions. For the cubic  $\text{CaSiO}_3$  perovskite, the situation is less complex. Our measurements indicate that under lower mantle conditions of pressure and temperature, the bulk modulus and density of  $\text{CaSiO}_3$  perovskite would be nearly identical to those of PREM. The role of  $\text{CaSiO}_3$  perovskite in the Transition Zone awaits further investigation.

**Acknowledgments.** We wish to thank D. H. Lindsley for starting material and M. T. Vaughan, R. C. Liebermann, J. Zhang, I. Martinez, and Y. Sinelnikov for their assistance during the experiments. We also thank D. Chapman, N. Lazarz, and W. Thomlinson of the X17 beamline at NSLS for their technical assistance. Comments made by Pascal Richet and an anonymous reviewer have significantly improved the manuscript. The SAM-85 project was supported by NSF grant EAR 89-20239 to the Center for High Pressure Research, State University of New York at Stony Brook. Mineral Physics Institute, State University of New York at Stony Brook, contribution 144.

## References

- Ahmed-Zaid, I., and M. Madon, A high-pressure form of  $\text{Al}_2\text{SiO}_5$  as a possible host of aluminum in the lower mantle, *Nature*, **353**, 426–428, 1991.
- Anderson, D. L., Composition of the Earth, *Science*, **243**, 367–370, 1989.
- Anderson, O. L., An experimental high-temperature thermal equation of state bypassing the Gruneisen parameter, *Phys. Earth Planet. Inter.*, **22**, 173–183, 1980.
- Anderson, O. L., A universal equation of state, *J. Geodyn.*, **1**, 185–214, 1984.
- Anderson, O. L., D. G. Isaak, and S. Yamamoto, Anharmonicity and the equation of state of gold, *J. Appl. Phys.*, **65**, 1534–1543, 1989.
- Anderson, O. L., D. Isaak, and H. Oda, High-temperature elastic constant data on minerals relevant to geophysics, *Rev. Geophys.*, **30**, 57–90, 1992.
- Decker, D. L., High-pressure equation of state for NaCl, KCl, and CsCl, *J. Appl. Phys.*, **42**, 3239–3244, 1971.
- Durben, D. J., and G. H. Wolf, High-temperature behavior of metastable  $\text{MgSiO}_3$  perovskite: A Raman spectroscopic study, *Am. Mineral.*, **77**, 890–893, 1992.
- Dziewonski, A. M., and D. L. Anderson, Preliminary reference Earth model, *Phys. Earth Planet. Inter.*, **25**, 297–356, 1981.
- Fei, Y., H. K. Mao, J. Shu, and J. Hu,  $P$ - $V$ - $T$  equation of state of magnesiowustite ( $\text{Mg}_{0.6}\text{Fe}_{0.4}\text{O}$ ), *Phys. Chem. Miner.*, **18**, 416–422, 1992.
- Funamori, N., T. Yagi, W. Utsumi, T. Kondo, and T. Uchida, Thermoelastic properties of  $\text{MgSiO}_3$  perovskite determined by in situ X ray observations up to 30 GPa and 2000 K, *J. Geophys. Res.*, in press, 1995.
- Gasparik, T., Transformations of enstatite-jadeite-diopside pyroxenes to garnet, *Contrib. Mineral. Petrol.*, **102**, 389–405, 1989.
- Gasparik, T., Phase relations in the transition zone, *J. Geophys. Res.*, **95**, 15,751–15,769, 1990.
- Gillet, P., P. Richet, F. Guyot, and G. Fiquet, High-temperature thermodynamic properties of forsterite, *J. Geophys. Res.*, **96**, 11,805–11,816, 1991.
- Horiuchi, H., E. Ito, and D. J. Weidner, Perovskite-type  $\text{MgSiO}_3$ : Single crystal X-ray diffraction study, *Am. Mineral.*, **72**, 357–360, 1987.
- Irifune, T., Absence of an aluminous phase in the upper part of the Earth's lower mantle, *Nature*, **370**, 131–133, 1994.
- Irifune, T., K. Fujino, and E. Ohtani, A new high-pressure form of  $\text{MgAl}_2\text{O}_4$ , *Nature*, **349**, 409–411, 1991.
- Jackson, I., and S. Rigden, Analysis of  $P$ - $V$ - $T$  data: Constraints on the thermoelastic properties of high-pressure minerals, *Phys. Earth Planet. Inter.*, in press, 1996.
- Kanzaki, M., J. F. Stebbins, and X. Xue, Characterization of quenched high pressure phases in  $\text{CaSiO}_3$  system by X-ray and  $^{29}\text{Si}$  NMR, *Geophys. Res. Lett.*, **18**, 463–466, 1991.
- Kudoh, Y., On the symmetry of the  $\text{CaSiO}_3$  perovskite quenched from 15 GPa and 1500 °C, paper presented at 14th AIRAPT Conference, Assoc. Int. for Res. and Adv. of High-Pressure Sci. and Technol., Colorado Springs, Colo., 1993.
- Liu, L. G., High-pressure phase transformations of albite, jadeite and nepheline, *Earth Planet. Sci. Lett.*, **37**, 438–444, 1978.
- Liu, L. G., and A. E. Ringwood, Synthesis of a perovskite-type polymorph of  $\text{CaSiO}_3$ , *Earth Planet. Sci. Lett.*, **14**, 1079–1082, 1975.
- Mammone, J. F., and S. K. Sharma, Pressure and temperature dependence of the Raman spectra of rutile-structured oxides, *Year Book Carnegie Inst. Washington*, **78**, 369–373, 1979.
- Mao, H. K., L. C. Chen, R. J. Hemley, A. P. Jephcoat, and Y. Wu, Stability and equation of state of  $\text{CaSiO}_3$  perovskite to 134 GPa, *J. Geophys. Res.*, **94**, 17,889–17,894, 1989.
- Mao, H. K., R. J. Hemley, J. Shu, L. Chen, A. P. Jephcoat, Y. Wu, and W. A. Bassett, Effect of pressure, temperature, and composition on the lattice parameters and density of  $(\text{Mg,Fe})\text{SiO}_3$  perovskite to 30 GPa, *J. Geophys. Res.*, **96**, 8069–8079, 1991.
- Meng, Y., D. J. Weidner, and Y. Fei, Deviatoric stress in a quasi-hydrostatic diamond anvil cell: Effect on the volume-based pressure calibration, *Geophys. Res. Lett.*, **20**, 1147–1150, 1993.
- Ringwood, A. E., and A. Major, Synthesis of majorite and other high pressure garnets and perovskites, *Earth Planet. Sci. Lett.*, **12**, 411–418, 1971.
- Tamai, H., and T. Yagi, High-pressure and high-temperature phase relations in  $\text{CaSiO}_3$  and  $\text{CaMgSi}_2\text{O}_6$  and elasticity of perovskite-type  $\text{CaSiO}_3$ , *Phys. Earth Planet. Inter.*, **54**, 370–377, 1989.
- Tarrida, M., and P. Richet, Equation of state of  $\text{CaSiO}_3$  perovskite to 96 GPa, *Geophys. Res. Lett.*, **16**, 1351–1354, 1989.
- Utsumi, W., N. Funamori, T. Yagi, E. Ito, T. Kikegawa, and O. Shimomura, Thermal expansivity of  $\text{MgSiO}_3$  perovskite under high pressures up to 20 GPa, *Geophys. Res. Lett.*, **22**, 1005–1008, 1995.
- Wang, Y., and D. J. Weidner, Thermoelasticity of  $\text{CaSiO}_3$  perovskite and implications for the lower mantle, *Geophys. Res. Lett.*, **21**, 895–898, 1994.
- Wang, Y., D. J. Weidner, and R. C. Liebermann, Thermal equation of state of  $(\text{Mg,Fe})\text{SiO}_3$  perovskite and constraints on composition of the lower mantle, *Phys. Earth Planet. Inter.*, **83**, 13–40, 1994.
- Weidner, D. J., and Y. Zhao, Elasticity and equation of state of perovskite: Implications for the Earth's lower mantle, in *High Pressure Research: Application to Earth and Planetary Sciences*, Geophys. Monogr. Ser., vol. 67, edited by Y. Syono and M. I. Manghni, pp. 191–196, AGU, Washington, D. C., 1992.
- Weidner, D. J., M. T. Vaughan, J. Ko, Y. Wang, X. Liu, A. Yeganeh-Haeri, R. E. Peralo, and Y. Zhao, Characterization of stress, pres-

- sure, and temperature in SAM85, a DIA type high pressure apparatus, in *High Pressure Research: Application to Earth and Planetary Sciences, Geophys. Monogr. Ser.*, vol. 67, edited by Y. Syono and M. H. Manghnani, pp. 13–17, AGU, Washington, D. C., 1992.
- Weidner, D. J., Y. Wang, and M. T. Vaughan, Yield strength at high pressure and temperature. *Geophys. Res. Lett.*, 21, 753–756, 1994.
- Zhao, Y., D. J. Weidner, J. B. Parise, and D. E. Cox, Thermal expansion and structural distortion of perovskite—Data for NaMgF<sub>3</sub> perovskite, I. *Phys. Earth Planet. Inter.*, 76, 1–16, 1993.
- Zhao, Y., J. B. Parise, Y. Wang, K. Kusaba, M. T. Vaughan, D. J. Weidner, T. Kikegawaa, J. Chen, and O. Shimomura, High-pressure crystal chemistry of neighborite, NaMgF<sub>3</sub>: An angle-dispersive diffraction study using monochromatic synchrotron X-radiation, *Am. Mineral.*, 79, 615–621, 1994.
- F. Guyot, Y. Wang, and D. J. Weidner, Center for High-Pressure Research and Department of Earth and Space Sciences, State University of New York at Stony Brook, Stony Brook, NY 11794-2100. (e-mail: ywang@sbmp04.ess.sunysb.edu)

(Received March 24, 1995; revised September 8, 1995; accepted October 17, 1995.)